A Multiloop System Stability Margin Study Using Matrix Singular Values

V. Mukhopadhyay* and J.R. Newsom†
NASA Langley Research Center, Hampton, Virginia

A stability margin evaluation method in terms of simultaneous gain and phase changes in all loops of a multiloop system is presented. A universal gain-phase margin evaluation diagram is constructed by extending an existing method using matrix singular value properties. Using this diagram and computing the minimum singular value of the system return difference matrix over the operating frequency range, regions of guaranteed stability margins can be obtained. Examples are presented for a wing flutter suppression and a drone lateral attitude control problem. The use of a return difference matrix eigenvalue plot in the complex plane is discussed.

Nomenclature

A,B,C,D	= control law quadruple matrices
F,G_u,H	= plant dynamics, input and output matrices, respectively
G	= open-loop transfer matrix
I	= identity matrix
j	$=\sqrt{-1}$
k_n	= nth loop gain in L matrix
L	= diagonal gain and phase change matrix
M	= order of control law
N_s,N_c,N_0	= order of plant, input, and output vectors, respectively
p	= a parameter
r	= reference signal
s	= Laplace variable
u	= plant input
x_c	= controller state vector
x_s	= plant state vector
z	= plant output vector
β	= sideslip angle (deg)
δ_1,δ_2	= elevon and rudder actuator state vectors, respectively (deg)
$\lambda(\ )$	= eigenvalue of matrix ( )
$\bar{\sigma}(\ ),\underline{\sigma}(\ )$	= maximum and minimum singular value, respectively, of matrix ( )
ϕ_n	= nth loop phase in L matrix (deg)
$\phi,\dot{\phi}$	= roll angle and rate (deg/s)
$\psi,\dot{\psi}$	= yaw angle and rate (deg/s)
ω	= frequency
$\|\ \|$	= magnitude of a scalar
$[\ ]^*$	= complex conjugate transpose of [ ]
$[\ ]^T$	= transpose of [ ]
$(\dot{})$	= represents time derivative of ( )

Introduction

ROBUSTNESS criteria of multi-input multi-output (MIMO) feedback control systems using matrix singular value properties and their relation to the classical gain and phase margins have been a subject of research in recent years.[1-4] In a multiloop system, the classical single-loop Nyquist tests are not adequate for stability margin evaluation since they consider the gain *or* phase change in one loop at a time. Using the minimum singular value of the system return difference matrix, criteria were developed in Ref. 4 for predicting guaranteed stability margins of multiloop systems in terms of either gain *or* phase change in all feedback loops. In this paper, the above method is extended to include simultaneous gain *and* phase change in all loops. A universal gain-phase margin evaluation diagram is constructed. Using this diagram and computing the minimum singular value of the system return difference matrix over the operating frequency range, regions of guaranteed gain and phase margins can be obtained. Using the singular value properties, one can develop an algorithm for a direct design of robust multiloop control laws using the concept of cumulative constraint.[5,6]

Singular values are computed for two examples for evaluation of their relation to stability margins. The first example is a 29th order single-input, single-output (SISO) system which represents an aeroelastic wind-tunnel wing model with a flutter suppression system. In Ref. 7, two flutter suppression control laws were synthesized that provided different degrees of robustness (gain and phase margins). These two control laws are examined using a classical Nyquist diagram and the singular value analysis. The correspondence between the stability margins predicted by the two methods is discussed.

The second example is an 8th order two-input, two-output system which represents an experimental drone aircraft[8] with a lateral attitude control system. The phase and gain margins from classical single-loop tests and the singular value approach are determined and compared with the stability boundary of the nominal system. The plot of the return difference matrix eigenvalue in the complex plane is also studied. This plot provides useful qualitative gain and phase margin information not contained in singular values.

Analysis

System Description

Let a multiloop feedback control system be described by the set of constant coefficient state-space equations expressed by Eqs. (1) to (4).

Plant

$$\dot{x}_s = Fx_s + G_u u \tag{1}$$

$$z = Hx_s \tag{2}$$

Presented as Paper 82-1574 at the AIAA Guidance and Control Conference, San Diego, Calif., Aug. 9-11, 1982; submitted Aug. 9, 1982; revision received July 29, 1983. This paper is declared a work of the U.S. Government and therefore is in the public domain.

*Scientist, NASA/GWU Joint Institute for Advancement of Flight Sciences. Member AIAA.
†Aerospace Engineer. Member AIAA.

Controller

$$\dot{x}_c = Ax_c + Bz \tag{3}$$

$$u = Cx_c + Dz \tag{4}$$

Equation (1) represents an N_sth order plant having N_0 output measurements z modeled by Eq. (2) and N_c control inputs u. Equations (3) and (4) represent an Mth order feedback control law driven by the sensor output z. The reference input signal $r=0$.

The system return difference matrix at the input is defined as $[I+G(s)]$ where

$$G(s) = -[C(Is-A)^{-1}B+D][H(Is-F)^{-1}G_u] \tag{5}$$

Here s is the Laplace variable. Figure 1 shows the block diagram of a multiloop system with unity feedback in which a square diagonal matrix L is introduced at the plant input u to examine the system gain and phase margins.

$$L = \text{Diag}[k_n \exp(j\phi_n)] \qquad n=1,2,\ldots,N_c \tag{6}$$

At nominal conditions, $k_n=1$ and $\phi_n=0$ for all n and, therefore, L is the identity matrix. In a traditional single-loop test, either k_n or ϕ_n is changed in one loop at a time. The gain or phase margin of the loop is defined as the smallest change in k_n or ϕ_n, respectively, from the nominal value for which the closed-loop system remains stable. The present objective is to find the range in which both k_n and ϕ_n can be changed simultaneously in all loops for which the system would remain stable.

Universal Gain and Phase Margin Diagram

The properties of singular values and their role in stability analysis of multiloop systems are discussed in detail in Refs. 1-4. Singular values of a matrix A are defined as the positive square root of the eigenvalues of A^*A. The minimum singular value of the nominal system (i.e., $L=I$) return difference matrix $\underline{\sigma}(I+G)$ is a measure of stability margin. In Ref. 4 it was shown that if the nominal system is stable, then the stability of the perturbed system is guaranteed if

$$\bar{\sigma}(L^{-1}-I) < \underline{\sigma}(I+G) \tag{7}$$

over all frequencies ($s=j\omega$). Note that this is a conservative condition, and it is possible to construct an L matrix which violates this condition, yet fails to destabilize the system.

Consider simultaneous gain and phase changes in every loop using the L matrix given by Eq. (6). Then

$$\bar{\sigma}(L^{-1}-I) = \max_n \sqrt{\left(1-\frac{1}{k_n}\right)^2 + \frac{2}{k_n}(1-\cos\phi_n)} \tag{8}$$

for all n with $k_n>0$. Reference 4 considers the classical cases of a gain change keeping $\phi_n=0$ and a phase change keeping $k_n=1$. Using Eq. (8), the general case of simultaneous gain and phase changes can be examined. Equation (8) is presented in Fig. 2 as a universal diagram for gain and phase margin evaluation. For example, if the smallest $\underline{\sigma}(I+G)$ for a system is 0.6, then the closed-loop system will tolerate simultaneous gain and phase changes of -1.5 dB to $+5.3$ dB, and -30 deg to $+30$ deg, respectively in all input loops. In a classical sense, when either gain or phase is changed, the gain margins are -4.2 dB and $+8$ dB ($\phi_1=\phi_2=0$), or the phase margins are $\pm 35°$ ($k_1=k_2=1$).

Using Eq. (8) the condition in Eq. (7) can be depicted as a plot of gain margin vs phase margin with the smallest $\underline{\sigma}(I+G)$ as a parameter. This is shown in Fig. 3 to indicate regions of guaranteed stability. If the phase and gain changes k_n and ϕ_n are within the elliptic stability regions for a particular $\underline{\sigma}(I+G)$, then the closed loop system must be stable.

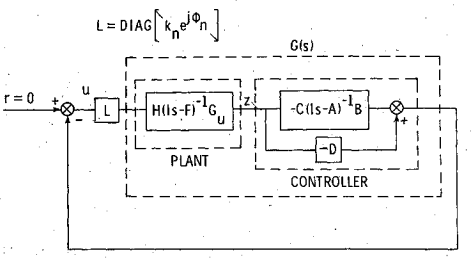

Fig. 1 Block diagram of multi-input, multi-output feedback control system with gain and phase change matrix at the input.

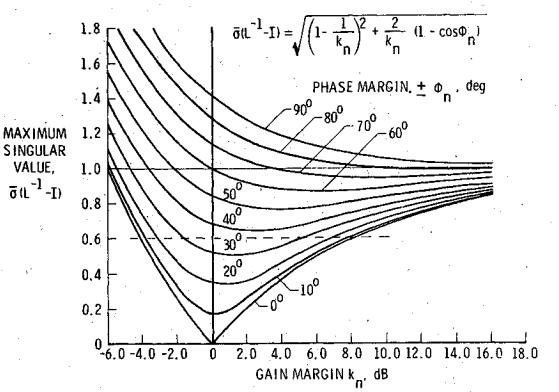

Fig. 2 Universal diagram for multiloop gain phase margin evaluation.

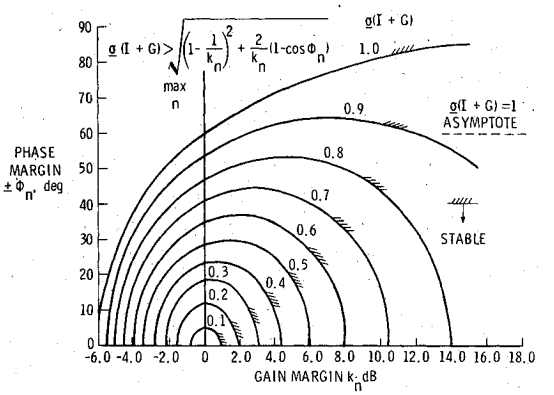

Fig. 3 Regions of guaranteed stability for various minimum singular value $\underline{\sigma}(I+G)$.

For example, if $\underline{\sigma}(I+G) \geq 0.7$ for all frequencies and ± 30 deg phase margins are required in all loops, then guaranteed simultaneous gain margins are -2.6 dB and $+8.5$ dB, i.e., both the phase and gain can be changed in all loops in any manner within these limits without destabilizing the closed loop system.

From Figs. 2 and 3, it is also easy to verify the well-known result that for a linear quadratic optimal state feedback problem the guaranteed gain margins are -6 dB and $+\infty$ dB and phase margins are ± 60 deg since $\underline{\sigma}(I+G) \geq 1$. When both gain and phase changes are considered for a given phase margin the corresponding gain margins can be established from Figs. 2 and 3.

Computation of Singular Value and Derivative

Since the frequency domain singular value analysis requires inversion of a (N_s+M)th order complex matrix of the type $(jI\omega-A)$ at a large number of frequencies, an efficient computational method[9,10] is used. The basic idea is to

transform A into an upper Hessenberg matrix so that for all ω, $(jI\omega - A)$ remains in upper Hessenberg form and the inversion problem can be solved quickly by simple forward and backward substitution. Thus, repeated upper and lower triangular transformations at each ω is avoided.

The complex matrix $(I+G)$ is of small order when multivariable systems involve only a few loops. It is possible to compute the singular value derivatives with respect to control law parameters with minimal additional computation and use them for direct design of robust multiloop control laws using optimization techniques with cumulative constraints.[5,6] The expressions for singular value derivatives are similar to those of eigenvalue derivatives and are presented in Appendix A.

Examples

Singular values are computed for two examples for evaluation of their relation to classical phase and gain margins. In the first example, involving a single-loop flutter suppression system,[7] the correspondence between the classical Nyquist diagram and the singular value plot is examined. Next a two-input, two-output system describing a drone aircraft[8] with a lateral attitude control system is analyzed.

29th Order Flutter Suppression System (SISO)

In Ref. 7, 4th order flutter suppression control laws were synthesized for a 25th order state space system representing an aeroelastic wind-tunnel wing model. Two control laws were synthesized that provided different stability margins. The transfer functions for these two control laws are:

Control Law (a)

$$\frac{u}{\ddot{z}} = \frac{(-364.4)(s-136.4)(s^2+73.69s+5697)}{(s+2.057)(s+2057)(s^2+46.37s+2047)} \frac{\text{deg}}{g}$$

Control Law (b)

$$\frac{u}{\ddot{z}} = \frac{(1939.4)(s+24.74)(s^2+87.63s+13806)}{(s+3.864)(s+3270)(S^2+20.97s+1423)} \frac{\text{deg}}{g}$$

Nyquist diagrams of the open loop transfer function $G(s)$ are presented in Fig. 4. For a SISO system this is the same as plotting the scalar $G(j\omega)$ in the complex plane. For Control Law (a) the gain margins are -4.1 dB and $+2.6$ dB and the phase margins are -22 and $+41$ deg. For Control Law (b) which is comparatively robust, the gain margins are -5.0 dB and $+12.3$ dB, and the phase margins are -53 and $+46$ deg.

A plot of the minimum singular value of $(I+G)$ as a function of frequency with Control Laws (a) and (b) are presented in Fig. 5. Since $(I+G)$ is a scalar, the minimum singular value is the absolute value of the scalar and the singular value plot gives the radial distance of the Nyquist locus from the critical -1 point in Fig. 4. The points A, B, C, and D on Fig. 5 correspond to the points on Fig. 4 where classical gain and phase margins are defined. If the singular values at points A, B, C, and D are used with Fig. 2, the gain and phase margins are determined to be identical to those determined from Fig. 4. However, the minimum singular value occurs at a slightly different point denoted by E. If the singular value at point E [0.23 for Control Law (a) and 0.69 for Control Law (b)] is used with Fig. 2 the guaranteed gain or phase margins are determined to be -1.8 dB, $+2.3$ dB, or ± 14 deg for Control Law (a) and -4.6 dB, $+10.2$ dB, or ± 40 deg for Control Law (b), respectively. When point E is located in the Nyquist locus in Fig. 4, the worst direction of simultaneous gain and phase change are found to be $+1.9$ dB and -8.0 deg for Control Law (a) and -3.3 dB and $+24$ deg for Control Law (b), respectively. These values can be verified using Fig. 2. For this example, the singular value-based stability margin predictions are realistic, particularly for the Control Law (b).

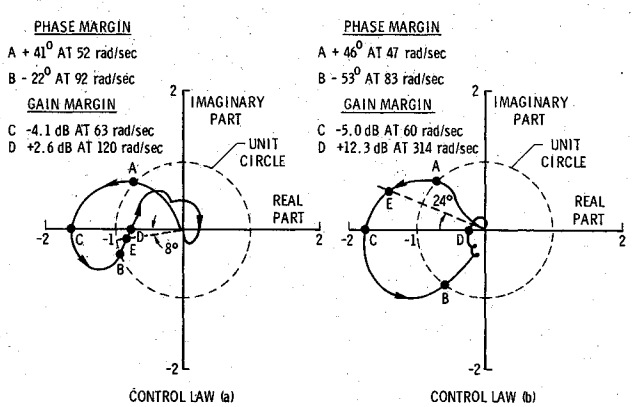

Fig. 4 Nyquist diagrams of 29th order flutter suppression system from Ref. 7 (arrows indicate increasing frequency).

8th Order Drone Lateral Attitude Control System (MIMO)

Figure 6 shows the block diagram of the lateral attitude control system of a drone aircraft.[8] The plant state vector x_s is defined as

$$x_s = [\beta,\ \dot{\phi}\ \dot{\psi},\ \phi\delta_1/20\ \delta_2/20]^T$$

The plant matrices, F, G_u, and H, as defined in Eqs. (1) and (2) are given in Table 1. The control law matrices A, B, C, and D as defined by Eqs. (3) and (4) are given in Table 2. The eigenvalues of the plant $\lambda(F)$ are given in Table 3. The eigenvalue at $\lambda = 0.1889 \pm j1.051$ results in an unstable Dutch Roll mode. the elements of the input vector $\{u_1 u_2\}^T$ are the elevon and rudder actuator servo commands, respectively. All gain and phase changes are considered at the points denoted by X in Fig. 6. Figure 7 shows the Nyquist diagrams from

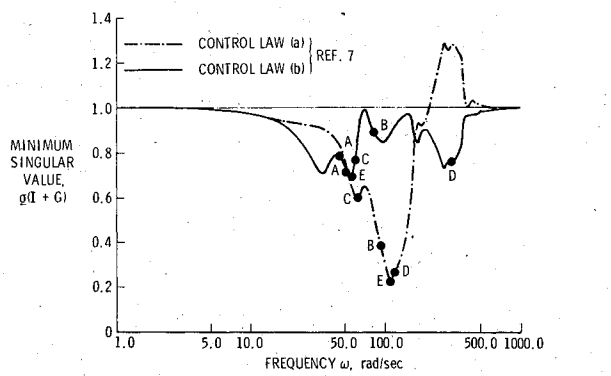

Fig. 5 Minimum singular value variation with frequency for 29th order flutter suppression system.

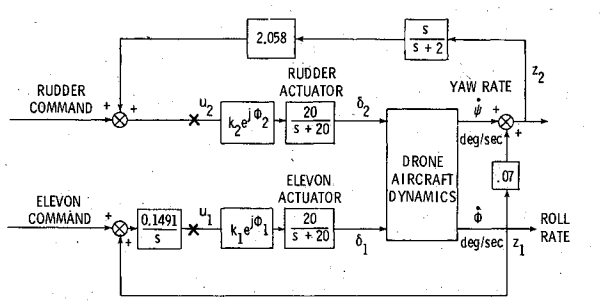

Fig. 6 Block diagram of a drone lateral attitude control system.

Table 1 Plant matrices F, G_u, and H for drone lateral attitude control system

$$F=\begin{bmatrix} -.08527 & -0.0001423 & -0.9994 & 0.04142 & 0 & 0.1862 \\ -46.86 & -2.757 & 0.3896 & 0 & -124.3 & 128.6 \\ -0.4248 & -0.06224 & -0.06714 & 0 & -8.792 & -20.46 \\ 0 & 1 & 0 & 0 & 0 & 0 \\ 0 & 0 & 0 & 0 & 20.0 & 0 \\ 0 & 0 & 0 & 0 & 0 & -20.0 \end{bmatrix}$$

$$G_u=\begin{bmatrix} 0 & 0 \\ 0 & 0 \\ 0 & 0 \\ 0 & 0 \\ 1 & 0 \\ 0 & 1 \end{bmatrix} \qquad H=\begin{bmatrix} 0 & 1 & 0 & 0 & 0 & 0 \\ 0 & 0.07 & 1 & 0 & 0 & 0 \end{bmatrix}$$

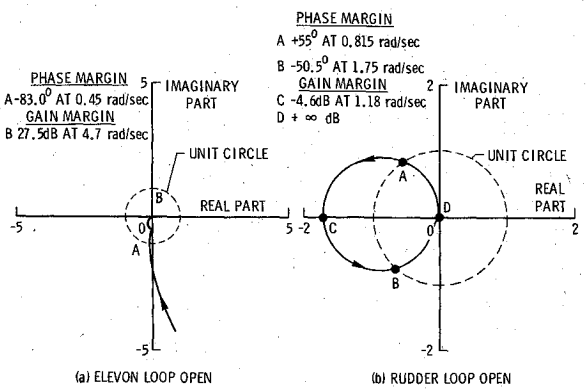

Fig. 7 Nyquist diagrams for single loop breaking tests (drone lateral attitude control sytem).

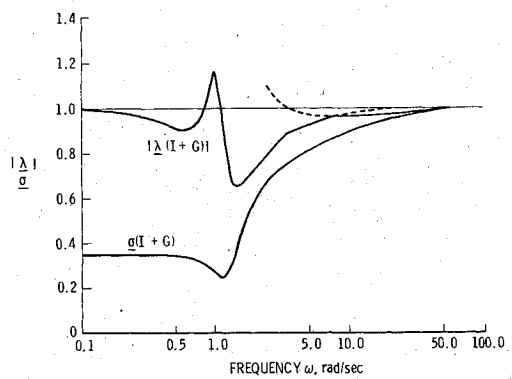

Fig. 8 Variation of minimum singular value (σ) and minimum eigenvalue ($|\lambda|$) of ($I+G$) with frequency (drone lateral attitude control system).

classical loop breaking tests at the elevon loop and rudder loop, respectively. From this diagram, the gain margin is 27.5 dB and the phase margin is -83.0 deg for the elevon loop designated as Loop 1. For the rudder loop, the gain margins are -4.6 dB and $+\infty$ dB, and the phase margins are $+55$ deg and -50.5 deg. This is the primary loop which stabilizes the Dutch Roll mode and is designated as Loop 2.

Although the single-loop values are often used as a measure of loop robustness, they may be inadequate to detect the overall system's weakness to simultaneous gain and phase changes in all loops. To study this for the present two-loop problem, the minimum singular value of the return difference matrix $\underline{\sigma}(I+G)$ over the operating frequency range is plotted

Table 2 Control law matrices A, B, C, and D for drone lateral attitude control system

$$A=\begin{bmatrix} 0 & 0 \\ 0 & -2 \end{bmatrix} \quad B=\begin{bmatrix} 1 & 0 \\ 0 & 1 \end{bmatrix}$$

$$C=\begin{bmatrix} 0.1491 & 0 \\ 0 & -4.116 \end{bmatrix} \quad D=\begin{bmatrix} 0 & 0 \\ 0 & 2.058 \end{bmatrix}$$

Table 3 The eigenvalues of the plant $\lambda(F)$

Plant	Eigenvalue
Spiral mode	-0.03701
Dutch roll (unstable)	$0.1889 \pm j1.051$
Roll convergence	-3.25
Elevon actuator	-20.0
Rudder actuator	-20.0

in Fig. 8. The minimum singular value is also the lower bound of the minimum eigenvalue magnitude $|\lambda(I+G)|$, which is also plotted in Fig. 8. The $\underline{\sigma}$ is constant at 0.35 over low frequencies, then drops to its lowest value of 0.25 near 1.2 rad/s, which is close to the frequency of the unstable open-loop pole. The $\underline{\sigma}$ increases sharply and approaches unity asymptotically as $G(j\omega)$ attenuates to zero at higher frequencies. Using the stability condition in Eq. (7), stability is guaranteed if $\bar{\sigma}(L^{-1}-I)<0.25$. Using Fig. 2, the guaranteed gain margins are found to be -2.0 dB and $+2.5$ dB. This means k_1 and k_2 can be changed from 0.8 to 1.33 (with $\phi_1=\phi_2=0$) in any manner without destabilizing the system. Similarly, ϕ_1 and ϕ_1 can be changed between -15 and $+15$ deg (with $k_1=k_2=1$) without encountering instability. If both gain and phase are changed, establish guaranteed gain margins can again be established for a given phase margin using Figs. 2 or 3. For example if the ϕ_1 and ϕ_2 variation is between -10 and 10 deg, the k_1 and k_2 can be varied between 0.85 and 1.23 with guaranteed stability.

These guaranteed stability boundaries are plotted as dashed line boxes in Fig. 9 as gain-stability boundaries denoted by P, Q, and R for the phase sets $\phi_1=\phi_2=0°$, $-10°$ and $-15°$, respectively. The last two ϕ_n perturbations are chosen in a critical direction towards instability (see Fig. 10, boxes Q and R, described later). Figure 9 also shows, in the solid line, the corresponding actual stability boundaries. These boundaries are established by plotting $\underline{\sigma}(I+G)$ for many k_n and ϕ_n values. On the boundary minimum $\underline{\sigma}(I+G)$ is zero. The

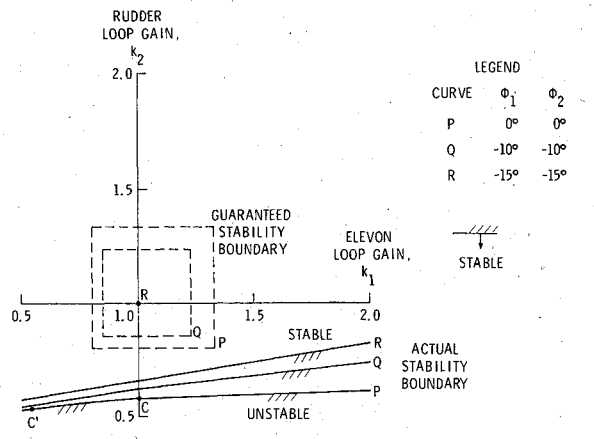

Fig. 9 Gain stability boundary for several phase perturbations at plant input based on minimum singular value and actual stability boundary.

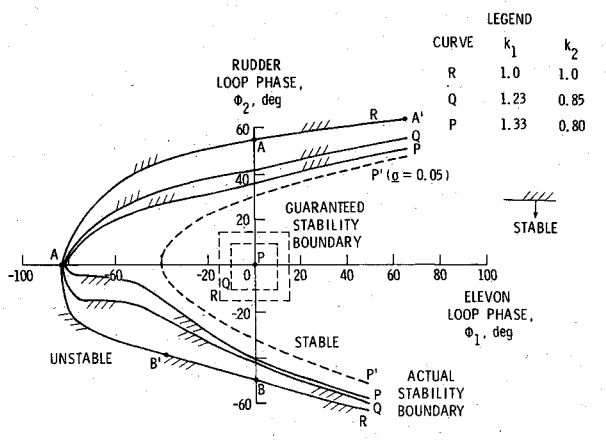

Fig. 10 Phase stability boundary for several gain perturbations at plant input based on minimum singular value and actual stability boundary.

boundary points are also verified from the origin encirclement pattern of the determinant and eigenloci of $(I+G)$.

Note that the classical loop breaking tests provide stability boundary points along the k_1 and k_2 axes (point C in Fig. 9 corresponding to point C in Fig. 7). The singular value analysis provides a somewhat conservative estimate of the stability margin when compared with the actual stability boundary.

In Fig. 10 the guaranteed and actual stability boundaries are shown as phase-stability boundaries denoted by R, Q, and P for the three gain sets $k_1=1.0$, $k_2=1.0$; $k_1=1.23$, $k_2=0.85$; and $k_1=1.33$, $k_2=0.8$. The last two sets of gain perturbations are chosen in a critical direction towards instability (see Fig. 9, corners Q and P). The corresponding guaranteed simultaneous phase margins are $\phi_1=\phi_2\pm15$ deg, ±10 deg, and 0 deg, respectively (boxes R and Q and point P in Fig. 10). The solid lines R, Q, and P denote actual stability boundaries. Note that the classical loop breaking tests provide stability boundary points along ϕ_1 and ϕ_2 axes (points A, A, B in Fig. 7 which corresponds to points A, A, B in Fig. 10). Although the Nyquist diagram presented in Fig. 7 predicted ample phase margins in individual loops, an examination of Fig. 10 indicates that if both ϕ_1 and ϕ_2 are changed in negative directions simultaneously, the system quickly becomes unstable in the vicinity of $\phi_1=-38$ deg, $\phi_2=-38$ deg, $(k_1=k_2=1)$, and at $\phi_1=-30$ deg, $\phi_2=-27$ deg $(k_1=1.23, k_2=0.85)$, and at $\phi_1=\phi_2=-25$ deg, $(k_1=1.33, k_2=0.8)$. To investigate the sensitivity of the actual boundary P the ϕ_1, ϕ_2 contour for $\underline{\sigma}=0.05$, $k_1=1.33$, and $k_2=0.8$ is also plotted as dashed line P', which indicates that the stability region shrinks rapidly with small changes in $\underline{\sigma}$ at these gain values. Although the singular value based predictions are conservative, they provide a good indication of the system's sensitivity to phase and gain perturbations.

In this example it is noted that some qualitative information about gain and phase margins can be obtained from the eigenvalues of $(I+G)$ matrix, which are plotted in the complex plane in Fig. 11. Note that the minimum eigenvalue magnitude $|\lambda(I+G)|$ plot in Fig. 8 represents the radial distance of the eigenvalue closest to the origin and is a measure of the closeness of $(I+G)$ to singularity in a limited sense, i.e., for equal diagonal perturbation in the L matrix. If k_1 and k_2 are reduced simultaneously to 0.54, the eigendiagram in Fig. 11 shrinks radially about the point 1.0 without rotation and point C' reaches the origin making the system unstable. Similarly, both k_1 and k_2 can be increased indefinitely without encountering instability. If ϕ_1 and ϕ_2 are changed simultaneously from zero to -38 deg, the diagram rotates about point 1.0 without distortion and point B' reaches the origin, making the system unstable. Likewise ϕ_1 and ϕ_2 can be increased simultaneously to $+65$ deg before

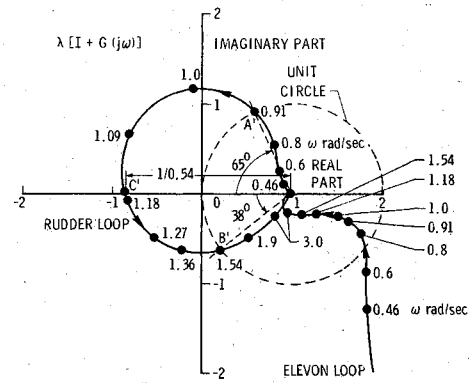

Fig. 11 Polar plot of eigenvalues of return difference matrix $\lambda(I+G)$ variation with frequency (drone lateral attitude control system).

point A' reaches the origin. These three specific stability boundary points correspond to points C', B', A' in the actual stability boundary in Figs. 9 and 10. Although nothing can be said regarding stability from Fig. 11 when gain or phase changes are unequal, it does provide qualitative information about the best and worst directions in gain or phase change. This useful design information cannot be obtained from singular value analysis.

Conclusions

A stability margin evaluation method for a multiloop system is presented by extending an existing procedure. The method involves computing the singular values of the system return difference matrix over the operating frequency range. The minimum singular value is related to the stability margins in terms of simultaneous gain and phase changes in all loops. Two examples are presented. In the first example involving a single loop flutter suppression system of a wing, the correspondence between the classical Nyquist diagram and the singular value plot is examined. In the second example, the stability of a two-loop lateral attitude control system of a drone aircraft is examined for simultaneous change in phase and gain. Although the singular value based predictions are generally conservative, they provide a good indication of the system's sensitivity to phase and gain perturbations. The eigenloci of the return difference matrix in the complex plane can indicate some qualitative phase and gain margin information to complement the singular value based stability margin analysis.

Appendix

Consider a general complex matrix G whose distinct singular values are σ_i, and whose corresponding right and left normalized eigenvectors are v_i and u_i, respectively. Hence by definition

$$Gv_i = u_i\sigma_i, \qquad G^*u_i = v_i\sigma_i \qquad i=1,2,\ldots N_c \quad \text{(A1,2)}$$

The normalized eigenvectors satisfy the following orthogonal properties

$$u_i^*u_j = \delta_{ij}, \qquad v_i^*v_j = \delta_{ij} \qquad \text{(A3)}$$

δ_{ij} is the Kroneker delta, which is unity when $i=j$ and zero when $i\neq j$. Let p be a real parameter for which derivative information is needed. Differentiating Eqs. (A1) and (A2) with respect to p and then premultiplying the result by u_i^* and v_i^*, respectively, and adding them together, obtains

$$u_i^*\frac{\partial G}{\partial p}v_i + v_i^*\frac{\partial G^*}{\partial p}u_i + (u_i^*G - v_i^*\sigma_i)\frac{\partial v_i}{\partial p} + (v_i^*G^* - u_i^*\sigma_i)\frac{\partial u_i}{\partial p} = \frac{\partial \sigma_i}{\partial p}(u_i^*u_i + v_i^*v_i) \qquad \text{(A4)}$$

Using Eqs. (A1-A3) in (A4), one obtains

$$\frac{\partial \sigma_i}{\partial p} = \frac{1}{2}\left(u_i^*\frac{\partial G}{\partial p}v_i + v_i^*\frac{\partial G^*}{\partial p}u_i\right) = \text{real part of } \left[u_i^*\frac{\partial G}{\partial p}v_i\right] \qquad \text{(A5)}$$

References

[1] Doyle, J.C. and Stein, G., "Multivariable Feedback Design: Concepts for a Classical/Modern Synthesis," *IEEE Transactions on Automatic Control,* Vol. AC-26, Feb. 1981, pp. 4-16.

[2] Postlethwaite, I., Edmunds, J.M., and Macfarlane, A.G.J., "Principal Gains and Principal Phases in the Analysis of Linear Multivariable Feedback Systems," *IEEE Transactions on Automatic Control,* Vol. AC-26, Feb. 1981, pp. 32-46.

[3] Safonov, M.G., Laub, A.J., and Hartmann, G.L., "Feedback Properties of Multivariable Systems: The Role and Use of the Return Diffference Matrix," *IEEE Transactions on Automatic Control,* Vol. AC-26, Feb. 1981, pp 47-65.

[4] Lehtomaki, N.A., Sandell, N.S., Jr., and Athans, M., "Robustness Results in Linear Quadratic Gaussian Based Multivariable Control Designs," *IEEE Transactions on Automatic Control,* Vol. 26, Feb. 1981, pp. 75-92.

[5] Greene, W.H. and Sobieszczanski-Sobieski, J., "Minimum Mass Sizing of a Large Low-Aspect Ratio Airframe for Flutter-Free Performance," *Journal of Aircraft,* Vol. 19, March 1982, pp. 228-234.

[6] Newsom, J.R. and Mukhopadhyay, V., "The Use of Singular Value Gradient and Optimization Techniques to Design Robust Controllers for Multiloop Systems," AIAA Paper No. 83-2191-CP, Aug. 1983.

[7] Mukhopadhyay, V., Newsom, J.R., and Abel, I., "A Method for Obtaining Reduced Order Control Laws for High Order Systems Using Optimization Techniques," NASA TP 1876, Aug. 1981.

[8] Perry, B., III, "Methodology for Determining Elevon Deflections to Trim and Maneuver the DAST Vehicle with Negative Static Margin," NASA TM 84499, May 1982.

[9] Laub, A.J., "Efficient Multivariable Frequency Response Computations," *IEEE Transactions on Automatic Control,* Vol. AC-26, April 1981, pp. 407-408.

[10] Peters, G., and Wilkinson, J.H., "Eigenvectors of Real and Complex Matrices by LR and QR Triangularizations," *Numerische Mathematik,* Vol. 16, 1970, pp. 181-204.